Online Appendix to "Short-term Planning, Monetary Policy, and Macroeconomic Persistence"*

Christopher Gust† Edward Herbst‡ David López-Salido§

January 2021

Abstract

This appendix provides additional details and results for the paper, "Short-term Planning, Monetary Policy, and Macroeconomic Persistence."

*The views expressed in this paper are solely the responsibility of the authors and should not be interpreted as reflecting the views of the Board of Governors of the Federal Reserve System or of anyone else associated with the Federal Reserve System.

†Federal Reserve Board. Email: christopher.gust@frb.gov

‡Federal Reserve Board. Email: edward.herbst@frb.gov

§Federal Reserve Board. Email: david.lopez-salido@frb.gov

This appendix contains additional results for the paper "Short-term Planning, Monetary Policy, and Macroeconomic Persistence." It also provides details about the data and methodology used to estimate the model.

1 Model Dynamics

This section contains additional results regarding the dynamic properties of the model with planning over finite horizons. It discusses the Taylor principle as well as the systems of equations determining the model's cycle and trend. It also shows that the model can generate a hump-shaped output response in response to a monetary shock without any need for habit persistence or the indexation of inflation to past values of inflation.

1.1 The Cycle and the Taylor Principle

The system determining the cycle is:

$$\tilde{x}_t = \rho M \cdot E_t[\tilde{x}_{t+1}] + N \cdot u_t, \tag{1}$$

where the matrices $M = \frac{1}{\delta}\begin{pmatrix} 1 & \sigma(1-\beta\phi_\pi) \\ \kappa & \kappa\sigma + \beta(1+\sigma\phi_y) \end{pmatrix}$ and $N = \frac{1}{\delta}\begin{pmatrix} -\sigma & -\sigma\kappa\phi_\pi \\ -\kappa\sigma & \kappa(1+\sigma\phi_y) \end{pmatrix}$, with $\delta = 1 + \sigma(\phi_y + \kappa\sigma_\pi)$. To determine the Taylor principle for the finite-horizon planning (FHP) model, rewrite the system (1) as

$$E_t[\tilde{x}_{t+1}] = A[\tilde{x}_t] + Bu_t,$$

where the relevant matrix A is given by

$$A = \begin{pmatrix} (\beta\rho)^{-1} & -\kappa(\beta\rho)^{-1} \\ \sigma(\phi_\pi - \beta^{-1}) & 1 + \sigma(\phi_y + \kappa\beta^{-1}) \end{pmatrix}.$$

The equilibrium is determinate if and only if the matrix A has both eigenvalues outside the unit circle (i.e., with modulus larger than one). Invoking proposition (C.1) in Woodford (2003), this condition is satisfied if and only if

$$\det(A) - tr(A) > -1.$$

This condition implies:

$$\left(\frac{1-\beta\rho}{\kappa}\right)\phi_y + \phi_\pi > \rho.$$

1.2 Trend-Cycle Decomposition

In this section, we report the matrices that determine the evolution of the model's trends. The evolution equations of v_t and v_{ft} are given by:

$$V_{t+1} = (I - \Gamma)V_t + \Gamma\Phi x_t, \tag{2}$$

where $V_t' = \begin{pmatrix} v_t & v_{ft} \end{pmatrix}$, and the matrices $\Gamma = \begin{pmatrix} \gamma & 0 \\ 0 & \gamma_f \end{pmatrix}$ and $\Phi = \begin{pmatrix} 1 & \sigma \\ 0 & \frac{1}{(1-\alpha)} \end{pmatrix}$. The trends can be written in terms of V_t as: :

$$\overline{x}_t = (1-\rho)\Theta V_t, \tag{3}$$

where the matrix of coefficients $\Theta = \frac{1}{\Delta}\begin{pmatrix} 1-\beta\rho & -\sigma(\overline{\phi}_\pi - \rho)(1-\alpha)\beta \\ \kappa & (1-\rho+\sigma\overline{\phi}_y)(1-\alpha)\beta \end{pmatrix}$ and $\Delta = (1 - \beta\rho)(1-\rho+\sigma\overline{\phi}_y) + \kappa\sigma(\overline{\phi}_{pi} - \rho)$.

Combining expression (2) with expression (3) yields:

$$\overline{x}_t = \Lambda \overline{x}_{t-1} + (1-\rho)\gamma Q x_{t-1},$$

where $\Lambda = \Theta(I-\Gamma)\Theta^{-1}$ and $(1-\rho)\gamma Q = \Theta\Gamma\Phi$. After some algebra these matrices can be written as:

$$\Lambda = \frac{1}{\Delta}\begin{pmatrix} (1-\gamma)(1-\beta\rho)(1-\rho+\sigma\overline{\phi}_y) + (1-\gamma_f)\frac{(\overline{\phi}_\pi-\rho)}{(\sigma\kappa)^{-1}} & \sigma(1-\beta\rho)(\overline{\phi}_\pi-\rho)(\gamma_f-\gamma) \\ (\gamma_f-\gamma)\kappa(1-\rho+\sigma\overline{\phi}_y) & (1-\gamma_f)(1-\beta\rho)(1-\rho+\sigma\overline{\phi}_y) + (1-\gamma)\frac{(\overline{\phi}_\pi-\rho)}{(\sigma\kappa)^{-1}} \end{pmatrix}$$

$$Q = \frac{1}{\Delta}\begin{pmatrix} (1-\beta\rho) & \sigma(1-\beta\rho) - \frac{\gamma_f}{\gamma}\sigma(\overline{\phi}_\pi-\rho)\beta \\ \kappa & \kappa\sigma + \frac{\gamma_f}{\gamma}(1-\rho+\sigma\overline{\phi}_y)\beta \end{pmatrix}.$$

When $\gamma = \gamma_f$, the system simplifies to:

$$\overline{x}_t = (1-\gamma)\overline{x}_{t-1} + (1-\rho)\gamma Q x_{t-1},$$

with $Q = \frac{1}{\Delta}\begin{pmatrix} 1-\beta\rho & \sigma(1-\beta\overline{\phi}_\pi) \\ \kappa & \kappa\sigma + (1-\rho+\sigma\overline{\phi}_y)\beta \end{pmatrix}$. Note that in this case the feedback of $\overline{x}_t$ on its lag can be characterized by the scalar, $1-\gamma$, and that Q is independent of γ. Finally, Q can be simplified further if $\overline{\phi}_y = 0$: $Q = \frac{1}{\Delta}\begin{pmatrix} 1-\beta\rho & \sigma(1-\beta\overline{\phi}_\pi) \\ \kappa & \kappa\sigma + (1-\rho)\beta \end{pmatrix}$, with $\Delta = (1-\beta\rho)(1-\rho) + \kappa\sigma(\overline{\phi}_\pi - \rho) > 0$ if $\overline{\phi}_\pi > \rho$.

1.3 Dynamic Responses to a Monetary Policy Shock

In this section we examine the impulse responses to a monetary policy shock to further illustrate the model's properties. In particular, we consider a tightening in policy, which corresponds to a positive innovation in $\epsilon_{i,t}$, for three different parameterizations. In the first, $\rho = 1.0$, which corresponds to the Canonical NK model in which the responses of the aggregate and cyclical variables are the same, and the model's trend corresponds to the nonstochastic steady state. In Figure 1, the Canonical NK model's impulse responses are labeled "Canonical NK". In the second and third parameterizations of the model, we set $\rho = 0.5$ which corresponds to 50 percent of households and firms doing their planning within the existing quarter, 25 percent of them doing it in two quarters, and only a small fraction – less than 0.5 percent – of households and firms having a planning horizon of two years or more. The second parameterization, labeled "Large gain" in Figure 1, sets $\gamma = 0.5$, which implies that households and firms put a relatively large weight on current observations in updating their value functions. The third parameterization, labeled "Small gain", is the same as the second one except that $\gamma = 0.05$. This value implies that current observations get a relatively small weight in the updating of agents' value functions.[1]

Figure 1 displays the impulse responses of output, y_t, inflation, π_t, and the short-term interest rates, i_t to a unit increase in $\epsilon_{i,t}$ at date 0. (All variables are expressed in deviation from their values in the nonstochastic steady state.) The first row in the figure corresponds to the responses of the aggregate variables, the second row to the trend responses, and the third row to the cyclical responses. As shown in the first row of the figure, a policy tightening results in an immediate fall in output of a little more than 2 percent and a 15 basis point fall in inflation in the Canonical model (green lines). Thereafter, the responses of output and inflation converge back monotonically to their steady state values. This monotonic convergence entirely reflects the persistence of the shock. The middle and lower panels of the figure confirm that in the Canonical model, there is no difference between the trends and steady state values of the model so that the aggregate and cyclical responses are the same.

[1] For these three cases, we set the remaining parameters as follows: $\beta = 0.995$, $\sigma = 1$, $\kappa = 0.01$, $\phi_\pi = 1.5$, $\phi_y = \frac{0.5}{4}$, and $\rho_{i^*} = 0.85$.

The blue lines, labeled "Large Gain," in Figure 1 show the impulse responses in the finite horizon model in which agents heavily weigh recent data in updating their value functions. As in the Canonical NK model, aggregate output and inflation fall on impact; however, the fall is dampened substantially. Moreover, output and inflation display hump-shaped dynamics despite the lack of indexation or habit persistence in consumption. While output reaches its peak decline after about a year, it takes substantially longer for inflation to reach its peak decline. As shown in the middle panel, these hump-shaped dynamics are driven by the gradual adjustment of the trends. The trend values for output and inflation fall in response to the policy tightening, reflecting that the policy shock persistently lower aggregate output and inflation. For output this return back to trend is relatively quick with a slight overshoot (not shown). However, the inflation trend returns back to its steady state very gradually as agents with finite horizons only come to realize slowly over time that the policy tightening will have a persistent effect on inflation.

The orange lines, labeled "Small Gain," show a similar parameterization except that agents update their value function even more slowly. In this case, the responses of the output and inflation trends is smaller and even more drawn out over time. Because of the dampened response of trend output, the response of aggregate output is no longer hump-shaped, as the aggregate effect is driven primarily by the monotonic cyclical response shown in the bottom left panel. In contrast, the aggregate inflation response is both dampened and more persistent. In sum, the finite horizon model is capable of generating substantial persistence in inflation and hump-shaped output responses following a monetary policy shock. Such dynamics are in line with empirical work examining the effects of monetary policy shocks on the macroeconomy.[2]

2 Data

The data used in the estimation is constructed as follows.

1. **Per Capita Real Output Growth.** Take the level of real gross domestic product (`FRED` mnemonic "GDPC1"), call it GDP_t. Take the quarterly average of the Civilian Non-institutional Population (`FRED` mnemonic "CNP16OV" / BLS series "LNS10000000"), call it POP_t. Then,

$$\begin{aligned}&\text{Per Capita Real Output Growth}\\ &= \quad 100\left[\ln\left(\frac{GDP_t}{POP_t}\right) - \ln\left(\frac{GDP_{t-1}}{POP_{t-1}}\right)\right].\end{aligned}$$

2. **Annualized Inflation.** Take the GDP deflator (`FRED` mnemonic "GDPDEF"), call it $PGDP_t$. Then,

$$\text{Annualized Inflation} = 400\ln\left(\frac{PGDP_t}{PGDP_{t-1}}\right).$$

3. **Federal Funds Rate.** Take the effective federal funds rate (`FRED` mnemonic "FEDFUNDS"), call it FFR_t. Then,

$$\text{Federal Funds Rate} = FFR_t.$$

The figures in the paper include two additional series, the CBO estimate of the Output Gap and longer-run inflation expectations. These data are constructed as follows.

1. **CBO Output Gap.** The CBO's estimate of the level of Potential GDP (`FRED` mnemonic "GDPPOT"), call it POT_t.

$$\text{CBO Output Gap}_t = 100\ln\left(\frac{GDP_t}{POT_t}\right).$$

[2] See, for instance, Christiano, Eichenbaum, and Evans (2005) and the references therein.

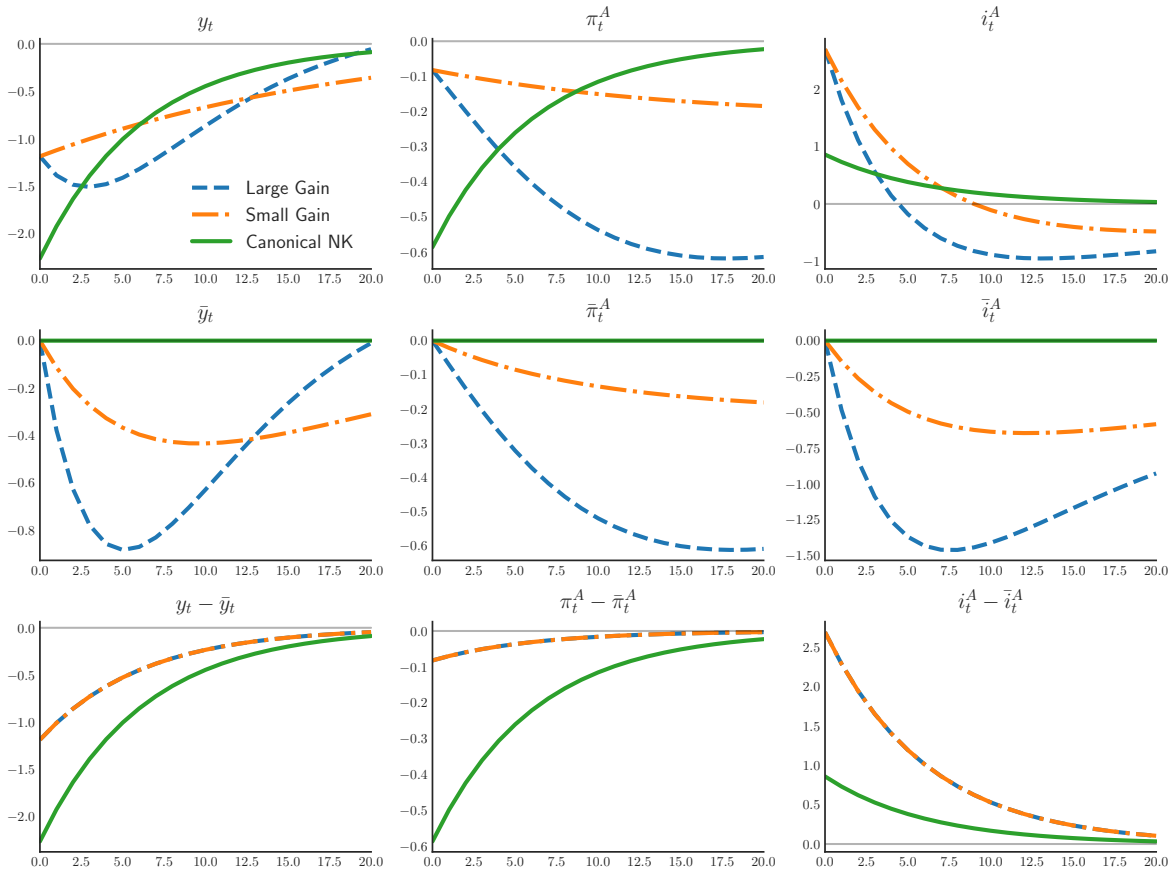

Figure 1: Impulse Responses to an Unexpected Monetary Tightening

NOTE: The figure shows impulse responses to a monetary policy shock. In the Canonical NK model (green lines), agents have infinite planning horizons ($\rho = 1.0$), and in the two remaining models, agents have finite planning horizons ($\rho = 0.5$). The first of these models, Large Gain (blue lines), agents update their value function quickly, ($\gamma = 0.5$); in the second one, Small Gain (green lines), agents update their value function slowly ($\gamma = 0.05$).

2. **Longer-run Inflation Expectations.** An estimate of historical inflation expectations can be found in the public FRB/US dataset. The variable is called PTR_t. Then,

$$\text{Longer-run Inflation Expectations} = PTR_t$$

2.1 Data Bibliography

Board of Governors of the Federal Reserve System (US), Effective Federal Funds Rate [FEDFUNDS], retrieved from FRED, Federal Reserve Bank of St. Louis; `https://fred.stlouisfed.org/series/FEDFUNDS`, July 31st, 2020.

Board of Governors of the Federal Reserve System (US), Long-run Inflation Expectations [PTR], retrieved from the Board of Governors of the Federal Reserve Systsem; `https://www.federalreserve.gov/econres/files/data_only_package.zip`, accessed November 24 2019.

Federal Reserve Bank of St. Louis, NBER based Recession Indicators for the United States

from the Period following the Peak through the Trough [USRECQ], retrieved from FRED, Federal Reserve Bank of St. Louis; https://fred.stlouisfed.org/series/USRECQ, January 5, 2021.

U.S. Bureau of Economic Analysis, Real Gross Domestic Product [GDPC1], retrieved from FRED, Federal Reserve Bank of St. Louis; https://fred.stlouisfed.org/series/GDPC1, July 31st, 2020.

U.S. Bureau of Economic Analysis, Gross Domestic Product: Implicit Price Deflator [GDPDEF], retrieved from FRED, Federal Reserve Bank of St. Louis; https://fred.stlouisfed.org/series/GDPDEF, July 31st, 2020.

U.S. Bureau of Labor Statistics, Population Level [CNP16OV], retrieved from FRED, Federal Reserve Bank of St. Louis; https://fred.stlouisfed.org/series/CNP16OV, July 31st, 2020.

3 Model Comparision: FHP-$\bar{\phi}$ and Hybrid NK Models

Parameter Estimates. In Table 1, we reproduce the posterior distributions of the FHP-$\bar{\phi}$ and the two Hybrid NK models. In this table, we include the median as well as the mean parameter values, as the posterior of the Hybrid NK model exhibits some bimodality. The estimated degree of habits in the Hybrid NK, governed by the parameter ν, is 0.93 at the posterior mean. By contrast, there is little evidence of indexation of prices, as the parameter a is near 1. Compared to the standard Hybrid NK model, the hybrid NK-λ_π model, with its *ad hoc* adjustment of the Fisher equation, yields similar estimates for price indexation parameter a, but a dramatically different estimate for habit formation parameter. In this model, the posterior mean estimate of ν is about 0.43, less than half its value in the Hybrid NK model. The Hybrid NK-λ_π features a very low estimate of λ_π, with $\lambda_\pi \approx 0.10$, indicating that the effect of expected future inflation on household spending is dampened considerably. Moreover, ϕ_y, which governs the response of the policy rate to the output gap, is about twice as large in the Hybrid NK-λ_π model as it is in the Hybrid NK model. Finally, the persistence and size of demand shocks are substantially higher in the Hybrid NK-λ_π model relative to the Hybrid NK model.

Posterior Predictive Checks. The estimates of the marginal data densities (MDD) in Table 5 in the main text provide summary measures of model fit, but these measures can sometimes be opaque. Here we supplement the MDD with *posterior predictive checks*. The logic of a (posterior) predictive check is simple. Let $\tilde{y}$ denote a random variable as distinguished from the realized value y, with $\mathcal{M}$ denoting a particular model. The posterior predictive distribution for $\tilde{y}$ under model $\mathcal{M}$ is given by

$$p(\tilde{y}|\mathcal{M}) = \int p(\tilde{y}|\theta, \mathcal{M}) p(\theta|Y, \mathcal{M}) d\theta. \tag{4}$$

Consider some statistic, $\mathcal{S}(y)$, of your data. Using (4), it is straightforward (at least conceptually) to compare where the observed statistic $\mathcal{S}(y)$ lies in the predictive distribution of a given model. Models for which important observed statistics of the data $S(y)$ lie in the tail of predictive distribution $S(\tilde{y}|\mathcal{M})$ are said to be deficient along a particular dimension. By comparing the posterior predictive distributions from two models, one can get a sense of the strengths and weaknesses of different models.

Figure 2 displays the posterior predictive distributions for the variance and first autocorrelation of output growth, as well as the covariance of output growth and inflation for each of the models, along with the observed values of these statistics. We choose these moments because the models display sizeable differences in predictions for them. Consider first the posterior predictive check for the variance of output growth. The Hybrid NK model predicts a counterfactually high variance for output growth, with the realized value falling in the tail of the distribution.

Table 1: Posterior Distributions of the FHP-$\bar{\phi}$ and Hybrid NK Models

	FHP-$\bar{\phi}$			Hybrid NK			Hybrid NK-λ_π		
	Mean	Median	SD	Mean	Median	SD	Mean	Median	SD
r^A	2.40	2.42	0.30	1.55	1.54	0.57	1.89	1.84	0.72
π^A	3.80	3.79	0.91	4.04	4.04	0.99	4.25	4.26	0.78
μ^Q	0.45	0.45	0.02	0.49	0.49	0.06	0.43	0.43	0.04
ρ	0.46	0.46	0.14						
γ	0.11	0.11	0.02						
ν				0.93	0.94	0.03	0.43	0.42	0.09
a				0.98	0.98	0.02	0.97	0.98	0.02
σ	3.72	3.69	0.65	1.47	1.43	0.41	1.79	1.75	0.47
κ	0.03	0.03	0.01	0.00	0.00	0.00	0.01	0.01	0.01
ϕ_π	0.94	0.92	0.15	1.64	1.63	0.23	1.65	1.64	0.25
ϕ_y	0.74	0.73	0.16	0.18	0.18	0.03	0.38	0.37	0.08
$\bar{\phi}_\pi$	2.09	2.08	0.26						
$\bar{\phi}_y$	0.06	0.04	0.05						
ρ_ξ	0.97	0.97	0.02	0.39	0.39	0.09	0.87	0.87	0.03
ρ_{y^*}	0.57	0.57	0.08	0.99	0.99	0.01	0.98	0.98	0.01
ρ_{i^*}	0.97	0.97	0.02	0.99	1.00	0.01	0.98	0.98	0.01
σ_ξ	2.08	2.02	0.39	0.93	0.92	0.08	2.89	2.73	0.93
σ_{y^*}	5.97	5.59	1.94	2.18	1.92	1.05	1.40	1.30	0.42
σ_{i^*}	0.58	0.56	0.11	0.49	0.48	0.06	0.53	0.53	0.06
Log MDD	-714.59	-714.61	0.10	-730.97	-730.98	0.11	-714.84	-714.88	0.08

NOTE: The table displays the mean, median, and standard deviation of the posterior distributions of parameters.

By contrast, both the FHP-$\bar{\phi}$ model and the Hybrid NK-λ_π model exhibit predictive distributions more consistent with the realized value in the data. The Hybrid NK model also fails to reproduce the negative correlation of output growth and inflation as well as the slightly positive autocorrelation in output growth. The Hybrid NK-λ_π model performs better (albeit it is still deficient) at reproducing the correlation of output growth and inflation, while succeeding at matching the persistence of output growth. For the autocorrelation of output growth, it outperforms even the FHP-$\bar{\phi}$ model. The differences between the two Hybrid NK models are tied to their respective estimates of ν, the habit parameter. The standard Hybrid NK model requires a large value for ν to match the correlation between inflation and the policy rate observed in the data. This high value for ν leads to output growth that is too highly autocorrelated, and a correlation between output growth and inflation that is too high relative to the data. By contrast, when the Fisher equation is broken—in an *ad hoc* fashion—the estimate of ν drops dramatically, and the persistence of output growth is in line with the data.

4 Posterior Sampler: Details and Additional Results

For most of the models in the paper, our estimation follows Herbst and Schorfheide (2014) with the following hyperparameters: $N_{part} = 16,000, N_\phi = 500, \lambda = 2.1, N_{blocks} = 3, N_{intmh} = 1$. We run each sampler $N_{run} = 10$ times, and pool the draws from the runs, yielding a posterior distribution with $160,000$ draws. There are three exceptions: for the Canonical NK, the Hybrid NK, and the FHP-$\tilde{\gamma}$ models, we use $N_{part} = 25,000$, $N_\phi = 2000$, and $N_{blocks} = 6$ because of bimodalities in the posterior.

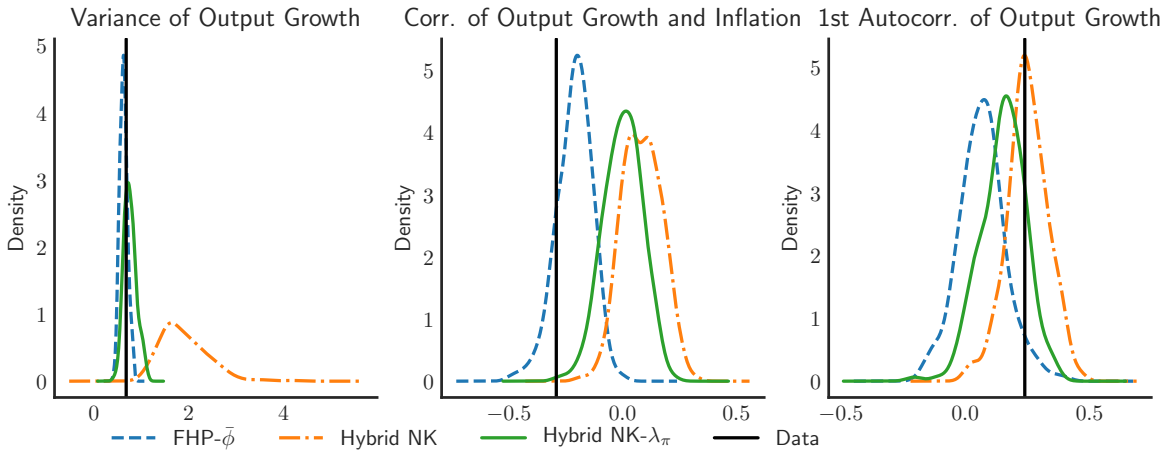

Figure 2: Posterior Predictive Checks

NOTE: The figure displays estimates of posterior predictive checks. The checks are computed by drawing from the respective posterior of each model $N = 200$ times and simulating, for each draw, observable datasets of length $T = 168$.

We assess the convergence and efficiency of our algorithm by analyzing the variation of the estimate of the sample mean across the N_{run} runs of the algorithm. This variance serves as an estimate of the CLT variance associated with the SMC-based estimate of the sample mean (as the number of particles becomes large). Call this estimated variance VAR$[\bar{\theta}]$ for any parameter θ. We also construct a measure of efficiency of the sampler based on the following idea: Suppose we were able to compute M *iid* draws from the marginal posterior distribution for θ. The variance of the mean, $\bar{\theta}$, of these draws would be given by

$$\mathbb{V}[\bar{\theta}] = \frac{\mathbb{V}[\theta]}{M},$$

where $\mathbb{V}[\theta]$ is the posterior variance of θ. We define the number of effective draws as:

$$\text{number of effective draws} = \frac{\hat{\mathbb{V}}[\theta]}{\text{VAR}[\bar{\theta}]},$$

where the hat indicates that we are using our estimated posterior variance. Such a measure indicates this (in)efficiency of the sampler, relative to hypothetical *iid* draws. Tables 2 through 9 display the estimated mean and 5th and 95th percentiles of the posteriors, in addition to the standard deviation of the mean across the N_{runs} runs and N_{eff}, the number of effective draws for each of the estimated models.

In general the SMC-based estimates of the posterior mean are relatively precise. The parameter σ_{y^*}, whose posterior mean lies in the tail of its prior distribution for many models, typically has the noisiest estimates. Across models, the Canonical NK model is the most difficult to estimate, owing to a bimodality in σ. However, this bimodality does not affect the stability of the estimate model fit (log MDD), as each mode has about the same density height.

Table 2: Posterior Distribution of the Canonical NK Model

	Mean	Std(Mean)	Q05	Q95	Neff
r^A	2.25	0.01	1.27	3.26	7060.56
π^A	3.76	0.01	2.55	5.03	6140.92
μ^Q	0.40	0.00	0.31	0.50	1764.48
σ	0.45	0.02	0.23	1.30	410.38
κ	0.31	0.01	0.01	0.49	539.78
ϕ_π	2.14	0.01	1.42	2.61	619.23
ϕ_y	0.10	0.01	0.00	0.95	393.38
ρ_ξ	0.93	0.00	0.80	0.97	348.04
ρ_{y^*}	0.99	0.00	0.95	1.00	491.94
ρ_{i^*}	0.71	0.00	0.62	0.96	524.75
σ_ξ	1.11	0.04	0.62	2.39	288.46
σ_{y^*}	1.18	0.06	0.81	2.44	783.37
σ_{i^*}	0.63	0.00	0.51	0.82	726.86

NOTE: The table displays the mean, 5th, and 95th percentile of the posterior distribution of the Canonical NK model, as well as the standard deviation of the posterior mean across 10 runs of the sampler.

Table 3: Posterior Distribution of the Exogenous Trends Model

	Mean	Std(Mean)	Q05	Q95	Neff
r^A	2.06	0.01	0.89	3.36	5815.27
π^A	3.88	0.03	2.46	5.30	942.33
μ^Q	0.43	0.00	0.38	0.47	2611.56
σ	1.75	0.01	1.08	2.57	1790.34
κ	0.00	0.00	0.00	0.00	2098.67
ϕ_π	1.57	0.00	1.17	2.01	3247.53
ϕ_y	0.86	0.00	0.60	1.21	2092.40
ρ_ξ	0.83	0.00	0.70	0.92	959.68
ρ_{y^*}	0.90	0.01	0.29	1.00	426.79
ρ_{i^*}	0.97	0.00	0.95	0.99	1767.18
σ_ξ	2.44	0.07	1.02	4.67	279.73
σ_{y^*}	1.58	0.03	0.75	3.15	807.21
σ_{i^*}	0.70	0.00	0.50	0.98	1895.24
$\rho_{\bar{\pi}}$	0.78	0.01	0.58	0.95	286.80
$\rho_{\bar{i}}$	0.96	0.00	0.90	0.99	1965.97
$\rho_{\bar{y}}$	0.95	0.00	0.86	1.00	3038.06
$\sigma_{\bar{\pi}}$	0.23	0.00	0.19	0.27	468.25
$\sigma_{\bar{i}}$	0.12	0.00	0.07	0.19	3742.10
$\sigma_{\bar{y}}$	0.12	0.00	0.07	0.19	1254.13

NOTE: The table displays the mean, 5th, and 95th percentile of the posterior distribution of the Exog. Trends model, as well as the standard deviation of the posterior mean across 10 runs of the sampler.

Table 4: Posterior Distribution of the FHP Model

	Mean	Std(Mean)	Q05	Q95	Neff
r^A	2.51	0.01	1.85	3.07	5251.54
π^A	3.98	0.01	2.34	5.62	6468.59
μ^Q	0.45	0.00	0.43	0.47	5544.45
ρ	0.50	0.01	0.27	0.71	639.00
γ	0.14	0.00	0.09	0.19	2192.39
σ	3.57	0.01	2.59	4.64	3790.00
κ	0.04	0.00	0.02	0.06	692.01
ϕ_π	1.07	0.00	0.89	1.30	6865.39
ϕ_y	0.79	0.01	0.57	1.07	926.28
ρ_ξ	0.98	0.00	0.94	1.00	4893.74
ρ_{y^*}	0.53	0.00	0.39	0.67	1533.31
ρ_{i^*}	0.97	0.00	0.95	0.99	5370.33
σ_ξ	2.17	0.02	1.62	2.94	515.89
σ_{y^*}	5.93	0.12	3.24	10.12	335.06
σ_{i^*}	0.67	0.00	0.51	0.89	1090.33

NOTE: The table displays the mean, 5th, and 95th percentile of the posterior distribution of the FHP model, as well as the standard deviation of the posterior mean across 10 runs of the sampler.

Table 5: Posterior Distribution of the FHP-$\tilde{\gamma}$ Model

	Mean	Std(Mean)	Q05	Q95	Neff
r^A	2.55	0.00	1.76	3.24	12107.09
π^A	3.96	0.01	2.34	5.59	19699.67
μ^Q	0.44	0.00	0.42	0.46	9307.94
ρ	0.69	0.00	0.47	0.85	915.59
γ	0.06	0.00	0.01	0.14	3165.49
$\tilde{\gamma}$	0.31	0.00	0.16	0.46	1650.56
σ	3.15	0.01	2.24	4.21	1719.39
κ	0.01	0.00	0.01	0.03	790.72
ϕ_π	1.01	0.00	0.78	1.29	15744.44
ϕ_y	0.93	0.00	0.65	1.30	3400.78
ρ_ξ	0.93	0.00	0.86	0.99	7124.87
ρ_{y^*}	0.31	0.00	0.14	0.51	1662.95
ρ_{i^*}	0.97	0.00	0.95	0.99	8313.81
σ_ξ	2.62	0.01	1.85	3.76	2125.10
σ_{y^*}	17.35	0.42	5.96	34.94	446.74
σ_{i^*}	0.77	0.00	0.56	1.06	4066.76

NOTE: The table displays the mean, 5th, and 95th percentile of the posterior distribution of the FHP-$\tilde{\gamma}$ model, as well as the standard deviation of the posterior mean across 10 runs of the sampler.

Table 6: Posterior Distribution of the FHP-$\bar{\phi}$ Model

	Mean	Std(Mean)	Q05	Q95	Neff
r^A	2.39	0.01	1.88	2.84	2243.90
π^A	3.80	0.01	2.33	5.33	3716.65
μ^Q	0.45	0.00	0.42	0.48	8951.67
ρ	0.46	0.01	0.22	0.68	525.70
γ	0.11	0.00	0.08	0.15	7959.75
σ	3.72	0.02	2.70	4.84	1001.96
κ	0.03	0.00	0.02	0.06	556.04
ϕ_π	0.94	0.00	0.71	1.20	9018.26
ϕ_y	0.75	0.00	0.53	1.03	1697.69
$\bar{\phi}_\pi$	2.09	0.00	1.68	2.52	3116.96
$\bar{\phi}_y$	0.05	0.00	0.00	0.16	4517.02
ρ_ξ	0.97	0.00	0.93	0.99	4036.74
ρ_{y^*}	0.57	0.00	0.45	0.70	1171.34
ρ_{i^*}	0.97	0.00	0.94	0.99	5604.30
σ_ξ	2.08	0.01	1.56	2.78	775.48
σ_{y^*}	5.99	0.11	3.64	9.61	308.57
σ_{i^*}	0.58	0.00	0.43	0.78	1970.05

NOTE: The table displays the mean, 5th, and 95th percentile of the posterior distribution of the FHP-$\bar{\phi}$ model, as well as the standard deviation of the posterior mean across 10 runs of the sampler.

Table 7: Posterior Distribution of the Angeletos-Lian Model

	Mean	Std(Mean)	Q05	Q95	Neff
r^A	1.83	0.02	0.69	3.26	1133.09
π^A	4.03	0.01	2.68	5.36	4850.55
μ^Q	0.41	0.00	0.38	0.45	3481.66
ρ	0.76	0.01	0.44	0.96	232.75
ρ_f	0.86	0.01	0.24	1.00	290.04
λ	0.08	0.00	0.01	0.22	3128.29
σ	1.88	0.01	1.10	2.79	2226.39
κ	0.03	0.00	0.01	0.12	290.52
ϕ_π	1.45	0.01	1.06	1.89	437.97
ϕ_y	0.51	0.01	0.25	0.85	214.24
ρ_ξ	0.87	0.00	0.81	0.94	1758.82
ρ_{y^*}	0.97	0.00	0.93	0.99	456.90
ρ_{i^*}	0.98	0.00	0.96	1.00	524.92
σ_ξ	0.36	0.00	0.30	0.44	239.75
σ_{y^*}	1.43	0.03	0.77	2.59	341.03
σ_{i^*}	0.56	0.00	0.44	0.75	546.13

NOTE: The table displays the mean, 5th, and 95th percentile of the posterior distribution of the Angeletos-Lian model, as well as the standard deviation of the posterior mean across 10 runs of the sampler.

Table 8: Posterior Distribution of the Hybrid NK Model

	Mean	Std(Mean)	Q05	Q95	Neff
r^A	1.55	0.04	0.64	2.51	205.42
π^A	4.04	0.01	2.41	5.67	15427.95
μ^Q	0.49	0.00	0.39	0.60	545.31
ν	0.93	0.00	0.87	0.97	209.17
a	0.98	0.00	0.94	1.00	7491.13
σ	1.47	0.01	0.86	2.21	2738.41
κ	0.00	0.00	0.00	0.00	189.17
ϕ_π	1.64	0.00	1.27	2.04	2838.78
ϕ_y	0.18	0.00	0.14	0.24	381.09
ρ_ξ	0.39	0.00	0.24	0.54	752.15
ρ_{y^*}	0.99	0.00	0.98	1.00	538.77
ρ_{i^*}	0.99	0.00	0.98	1.00	261.51
σ_ξ	0.93	0.00	0.82	1.07	814.29
σ_{y^*}	2.18	0.04	1.10	4.15	772.22
σ_{i^*}	0.49	0.00	0.40	0.59	5578.19

NOTE: The table displays the mean, 5th, and 95th percentile of the posterior distribution of the Hybrid NK model, as well as the standard deviation of the posterior mean across 10 runs of the sampler.

Table 9: Posterior Distribution of the Hybrid NK-λ_π Model

	Mean	Std(Mean)	Q05	Q95	Neff
r^A	1.89	0.01	0.81	3.17	14242.89
π^A	4.25	0.01	2.94	5.51	7721.07
μ^Q	0.43	0.00	0.37	0.49	3806.14
ν	0.43	0.00	0.29	0.57	3297.41
a	0.97	0.00	0.92	1.00	15047.89
λ_π	0.10	0.00	0.01	0.24	6389.45
σ	1.79	0.01	1.09	2.64	4650.79
κ	0.01	0.00	0.00	0.02	1352.43
ϕ_π	1.65	0.00	1.26	2.07	5824.27
ϕ_y	0.38	0.00	0.26	0.52	2786.47
ρ_ξ	0.87	0.00	0.81	0.92	2074.63
ρ_{y^*}	0.98	0.00	0.95	1.00	5497.73
ρ_{i^*}	0.98	0.00	0.96	1.00	1557.50
σ_ξ	2.89	0.03	1.69	4.62	1085.26
σ_{y^*}	1.40	0.01	0.94	2.18	798.35
σ_{i^*}	0.53	0.00	0.45	0.63	7079.41

NOTE: The table displays the mean, 5th, and 95th percentile of the posterior distribution of the Hybrid NK-λ_π model, as well as the standard deviation of the posterior mean across 10 runs of the sampler.

Figure 3: Estimated Innovations

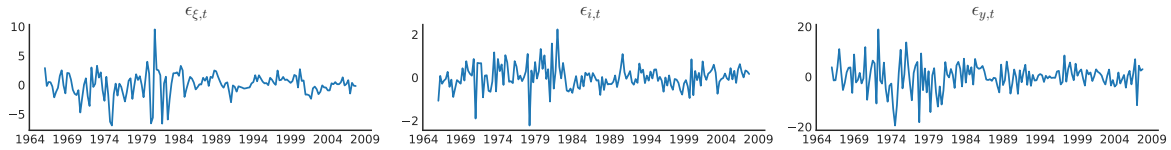

NOTE: The figure shows the time series of the posterior mean smoothed innovations for the FHP-$\bar{\phi}$ model.

References

Christiano, L. J., M. Eichenbaum, and C. L. Evans (2005): "Nominal Rigidities and the Dynamic Effects of a Shock to Monetary Policy," *Journal of Political Economy*, 113(1), 1–45.

Herbst, E., and F. Schorfheide (2014): "Sequential Monte Carlo Sampling for DSGE Models," *Journal of Applied Econometrics*, 29(7), 1073–1098.

Woodford, M. (2003): *Interest and Prices Foundations of a Theory of Monetary Policy*. Princeton University Press, Princeton, NJ.